Experimental Configuration and Preliminary Results of Testing a Rapid Cycle Adsorption Pump for Martian CO_2 Acquisition

Jared Berg[1], Anthony Iannetti[2], and Hashmatullah Hasseeb[3]
NASA Glenn Research Center, Cleveland, OH, 44135

Temperature-swing adsorption pumps have been proposed as a method of acquiring and compressing Martian atmospheric CO_2 for downstream processing. Most industrial applications and previous research targeted at space in-situ resource utilization (ISRU) utilize long (~hours) temperature swing periods, typically limited by the ability to transfer heat from a naturally insulating sorbent bed. A rapid cycle adsorption pump (RCAP) would reduce these periods to minutes, in the hope of increasing overall throughput. This paper details the design and preliminary experimental results from testing an RCAP in a simulated Martian environment. The test configuration features a central, liquid-cooled and heated heat transfer plate surrounded by symmetrical rectangular sorbent beds. Various bed thicknesses and commercially available Zeolite 13X sorbent particle sizes will be evaluated to both determine performance and provide data for a parallel modeling effort. Discussions of multi-stage configurations and considerations regarding bed conductivity are included.

Nomenclature

ISRU	=	In-Site Resource Utilization
MACS	=	Mars Atmospheric Chemistry Simulator
RCAP	=	Rapid Cycle Adsorption Pump

I. Introduction

RELYING on local resources to generate life support and propulsion commodities holds the promise of reducing the launch mass requirements of a Mars mission and paving the way for long term settlement. However, any technology that becomes a piece of critical infrastructure must be both robust and efficient. To effectively harvest the resource of Martian atmospheric CO_2 for downstream processes, it must be compressed from a low ambient pressure of ~7 Torr to ~10^2-10^3 Torr. Mechanical compressors are capable of this, but concerns about the long-term reliability of high-speed moving parts and overall energy requirements have prompted work on alternative compression methods.

Adsorption is a physical or chemical process where a fluid species preferentially bonds with the surface of a solid sorbent, and is dependent on pressure and temperature. Sorbents are highly porous on the micro scale with a large specific surface area, and can be tuned to selectively bond with a particular species. Therefore, an adsorption process can concentrate a target species far beyond its initial density.
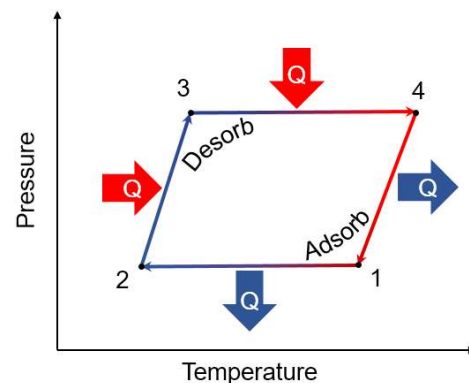

Figure 1. Ideal temperature-swing adsorption cycle.

An ideal thermodynamic cycle for a temperature-swing adsorption process is depicted in Figure 1. During process (1-2) the pump is open to the atmosphere and adsorbing while heat is removed from the sorbent. At state (2) the pump volume is isolated and heated to state (3) in order to increase pressure. From state (3) to (4), heating continues as gas is allowed to leave the pump at constant pressure. The volume is again closed at state (4) and the bed is recooled to state (1), ready for the cycle be begin again. Either with storage tank or multiple RCAPs in parallel, continuous CO_2 supply may be achieved.

Separation and purification of gases by adsorption is a common industry practice[1], and adsorption pumps have long been proposed for Mars missions[2,3] due to their relative mechanical simplicity and ability to utilize waste heat and environmental heat sinks. The typical duration of a temperature swing cycle has been on the order of hours, due both to the thermal mass of the necessary sorbent and an attempt to exploit diurnal temperature variation[4]. More recent work has suggested that relatively rapid cycling (~minutes) of the sorbent temperature could yield overall higher production rates[5-7], yielding the creatively named Rapid Cycle Adsorption Pump (RCAP).

Rapid cycling highlights the limits on heat and mass transfer inherent in the adsorption pump concept and introduces many complex trades between various design features. Sorbents tend to have low thermal conductivity due to their high porosity and are traditionally manufactured as pellets for use in packed beds, where limited inter-pellet contact and wall-packing effects further impede conduction. Various attempts to boost bed conductivity have been made[8,9] but no solution seems obviously superior, in part due to the fact that any high-conductivity material added to a given design displaces bed volume that alternatively could be occupied by sorbent. Said another way, it is challenging to find an optimal balance between increasing the ability to swing the temperature of a certain quantity of sorbent and just adding more sorbent. Despite the disadvantages of packed beds for heat transfer, their inherent macro-porosity is suited to mass transfer of fluid species. This is important because of the difficulty of moving the low pressure ambient atmosphere throughout a pump apparatus. Different methods of packaging the pump, choice of heat transfer fluids, and whether the RCAP should have multiple stages are all critical questions with interrelated answers, often dependent on higher-level ISRU architecture choices.
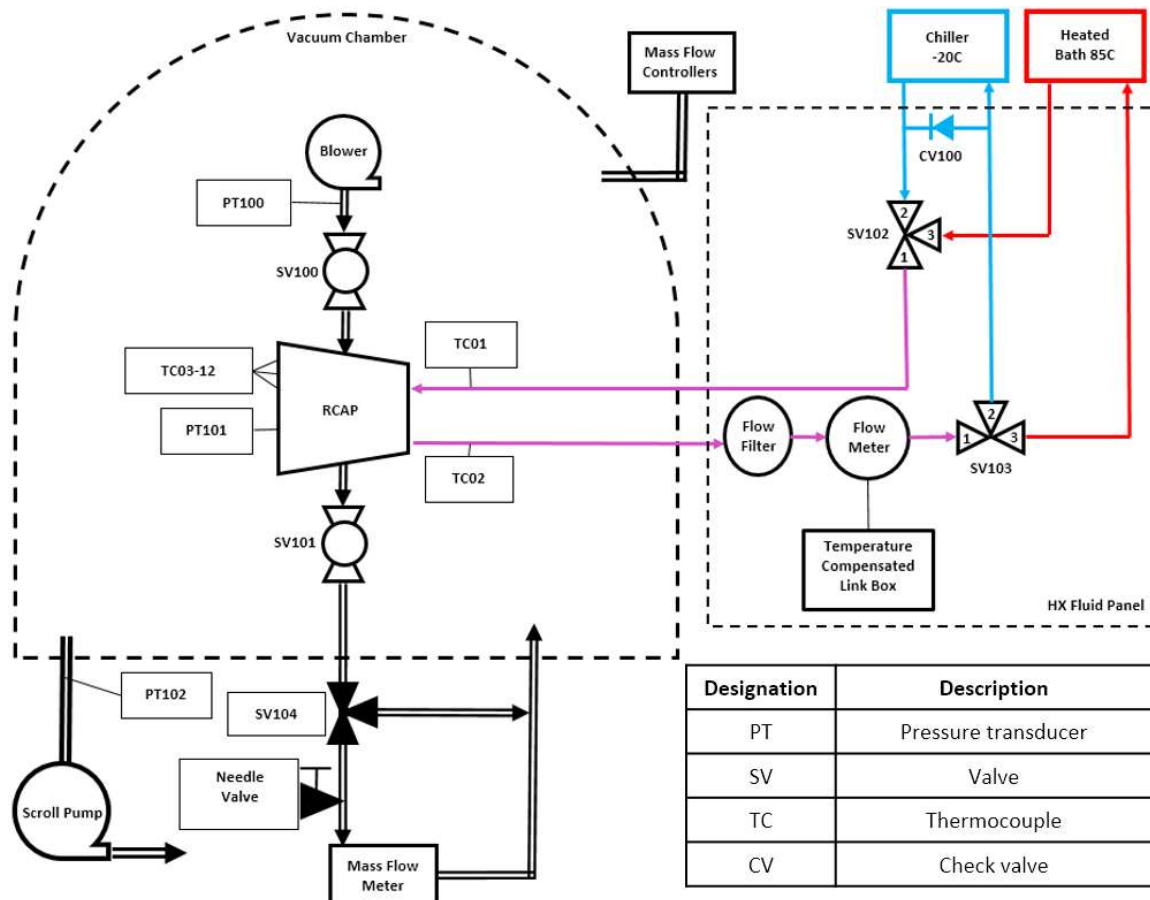

Figure 2. Experimental setup schematic.

Tackling these optimization challenges and constructing a reliable, human-mission scale pump will require more powerful modeling techniques and a thorough experimental campaign. The RCAP discussed here is a second step in the direction of this goal. It is a larger-scale prototype than previous configurations[7]. It aims to collect data useful for a parallel modeling effort. Enhanced models will allow further scaling to match NASA's current ISRU commodity production goal[10].

II. Test Setup

A. Facility and Ancillary Hardware

Figure 2 depicts the experimental configuration in schematic form. Testing was performed in the Mars Atmospheric Chemistry Simulator (MACS) chamber at NASA Glenn Research Center. The MACS is a 200 L volume stainless steel bell jar, with two side viewing ports and nine feedthrough ports in the base. It also features connections for gas and fluid exchange. The chamber is evacuated by a Varian TriScroll 600 roughing pump, connected in parallel with an Alicat PCR pressure controller. Supply gas can be bled into the chamber at a constant rate through three parallel Alicat mass flow controllers while the pressure controller modulates the applied vacuum yielding a simulated Martian atmosphere of 95% CO_2, 2.7% N_2, and 1.6% Ar at 6-9 Torr. The temperature of the chamber walls or the supply gas is not controlled and is assumed to correspond to the room temperature of 23° C.

Pressure is measured inside the chamber at multiple locations. There are two Setra ASM pressure transducers (visible in Figure 3), one mounted outside the RCAP body that essentially monitors chamber pressure (plus the tiny pressure rise caused by the inlet-side blower) and one incorporated in the RCAP itself measures the pump pressure. There is also a pressure signal from the Alicat pressure controller located upstream of the scroll pump. The outlet of the RCAP is routed outside the chamber, and can be selectively channeled through either an Alicat MS-series mass flow meter or a bypass line via an ASCO 3-way solenoid valve, back into the chamber.

The RCAP utilizes a liquid-solid heat exchanger, as discussed below, which is supplied by separate heated and chilled baths. The heated bath is a Fisher Scientific Isotemp 5150 H7, which features an internal centrifugal circulation pump and an open bath. The chiller is an SP Scientific RC311, which is sealed and also has an internal pump. Both are visible in the periphery of Figure 4, along with previously mentioned components. The chosen heat exchange liquid was 3M Fluorinert FC-770. Fluorinert is widely used as a high-performance heat transfer fluid in the electronics industry because it is non-conductive, has wide material compatibility, a broad operating temperature range, and leaves no residue. Similar fluorinated liquids have been used previously in spaceflight applications. The main disadvantage of FC-770 is its relatively high cost.

Both the heater and chiller are plumbed beneath the MACS chamber (Figure 4), where Swagelok SS-44XTS
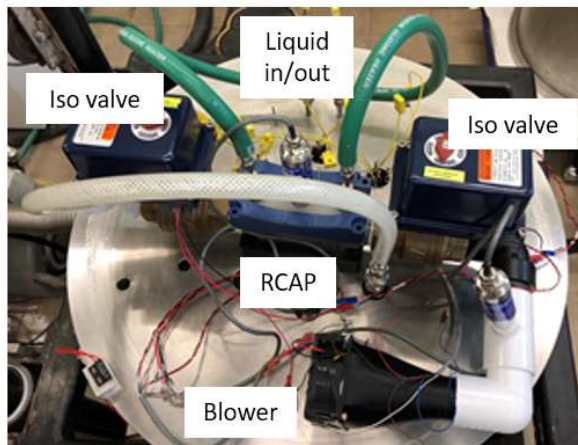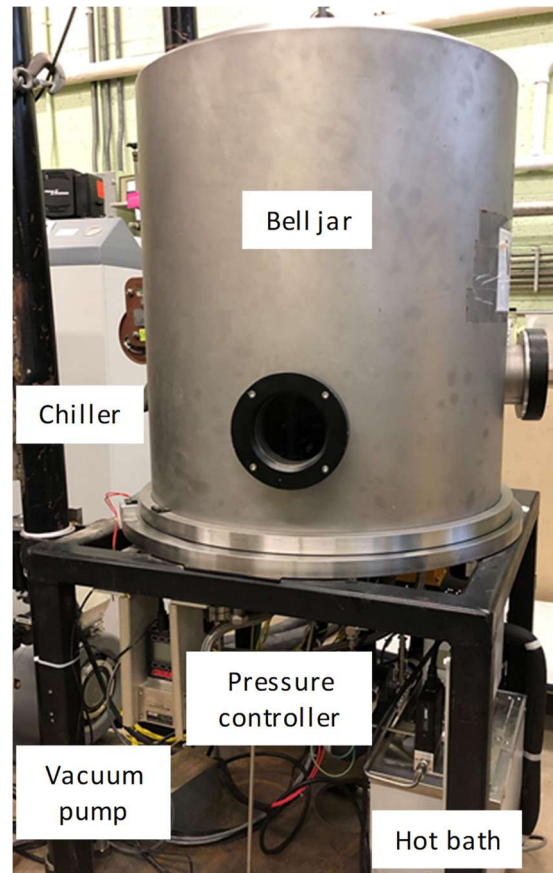

Figure 3. RCAP test configuration.
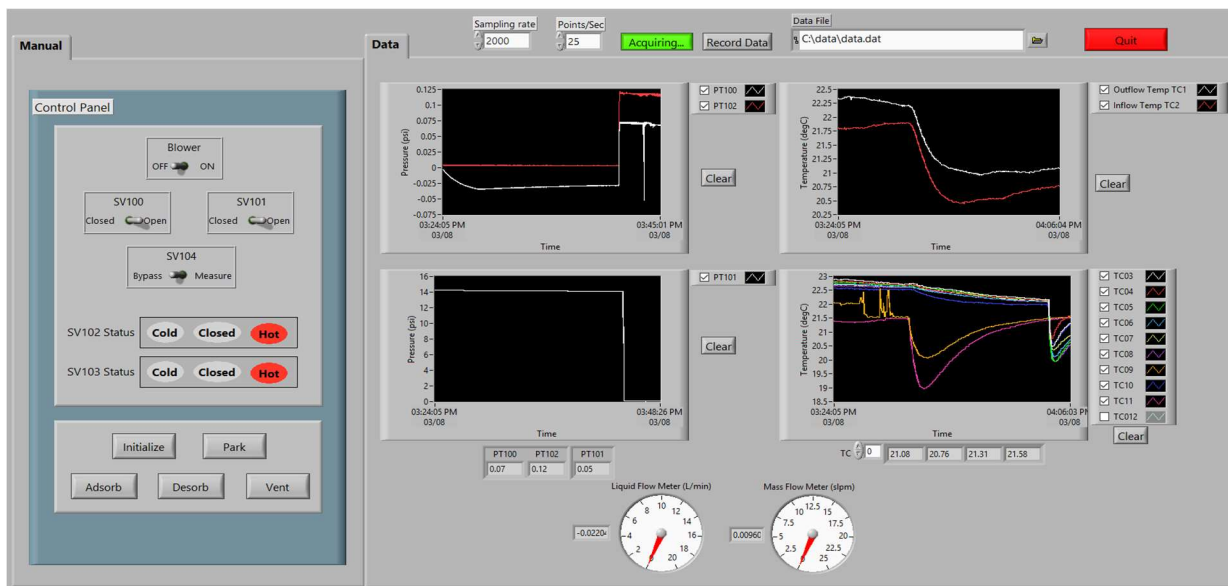

Figure 4. MACS chamber exterior.

Figure 5. LabVIEW interface.

DC-actuated 3-way valves can selectively supply and return the liquid to the appropriate bath. The fluid flow rate is measured upon return from the RCAP by a Flow Technology FT8 turbine flow meter paired with a Temperature Compensated Link interface calibrated for FC-770. Temperature data is collected at the liquid inlet and outlet of the chamber, and at multiple locations throughout the RCAP sorbent bed.

The system is controlled via a LabVIEW interface (Figure 5) with a National Instruments cDAQ-9178 chassis that includes NI 9205 analog input, NI 9482 power relay, and NI 9213 thermocouple cards. The interface allows manual or semi-autonomous control of the whole pump cycle, enabling repeatable, multi-hour tests to evaluate RCAP performance.

B. Pump Configuration

The geometry of the RCAP, seen in exploded form in Figure 6, was determined by balancing a few different factors: functional scale, ease of modeling correlation, and fabrication and operational simplicity. Functional scale refers to both the amount of sorbent present in the pump, which in this RCAP is 50-250 g, and the size of the sorbent bed relative to the constituent media (pellets). A flight scale unit will feature kilograms of sorbent in order to achieve desired production rates, and the design and packaging of this unit will be

Figure 6. RCAP exploded view.

crucial for specific productivity (rate of CO_2 production / mass of required hardware) and energy efficiency. Packaging is a more dominant fraction of the total system mass at small scale, therefore previous small-scale tests (e.g. < 10 g sorbent), while useful for proof of concept, have a limited relationship to flight. Also, sorbent media usually come as pellets of various types, the size of which may have important impacts on overall performance[11,12]. The pellet / bed size ratio will determine bed voidage[13], with effects on mass efficiency and heat and mass transfer. As with any development project, the closer one gets to final scale the more relevant the conclusions become.
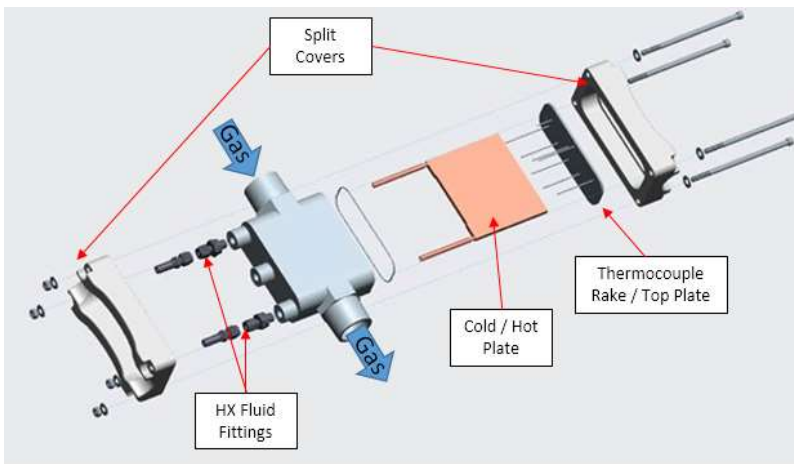
Model correlation is a key motivation of this experiment, so a choice of geometry that limits the unknown modeling parameters and approximates theoretical boundary conditions is preferable. We decided on a flat heat exchanger plate with sorbent symmetrically distributed on either side and gas flowing perpendicular to the dominant direction of heat transfer. This configuration shares many features with analytical solutions of heat transfer in porous media[14], and the simple geometry is easy to model numerically. With improved and experimentally verified[15] correlations for predictive modeling in hand, future designs would incorporate higher-performance geometry.

To facilitate experimental operations, limit the potential for leaks, and gain familiarity with modern 3D printing capability, we designed a pump housing that could be created as a single unit. The housing was printed from an aluminum-silicon alloy, and incorporates outlets for gas and liquid exchange, internal pellet retention features, slots for "blanking volumes" that adjust the bed thickness and pump free volume, and a sealing top cover with an integrated thermal rake, all seen in Figure 7. Finish machining included cutting threads and smooth mating surfaces. The rakes were made of hollow stainless steel to minimize conductivity, with Omega K-type thermocouples potted at each tip with conductive epoxy.

The heat exchanger plate was manufactured in traditional fashion from copper, with four parallel internal "mini-channels" and mated to the housing with Swagelok fittings. It floats in the housing with minimal contact to avoid adding the rest of the pump exterior as a coupled

Figure 7. RCAP housing and covers. *(Top) Housing with heat exchanger plate and blanking volumes installed and O-ring groove visible, (bottom) three top plates with differing thermocouple rake arrangements corresponding to bed size.*

thermal mass. Originally, the plate was of a different design and printed as an integral piece of the housing, but thermal stresses from printing led to crack formation during finishing. Despite that failure, if new geometries for optimizing heat transfer are developed that exceed the capabilities of subtractive techniques, 3D printing shows much promise.

The first stage of the RCAP shown in Figure 7 features large diameter gas passages to reduce any flow restrictions that may occur with such a low density ambient atmosphere. To isolate the pump volume during desorption, two Dynaquip 1.5" (3.81 cm) internal diameter electrically-actuated ball valves are attached at each end of the housing.

III. Experimental Parameters

Heat and mass transport in the sorbent bed determine the performance of an RCAP, so we targeted these factors specifically in this test series. These transport mechanisms are most strongly controlled by the sorbent type, its physical arrangement in the bed, and the size of the bed. This investigation looked at commercially available Zeolite 13X from Strem Chemical in three different formats: 1/8" (3.18 mm) diameter cylindrical pellets, 1/16" (1.59 mm) diameter cylindrical pellets, and 600 mesh powder, as depicted in Figure 8. In general, larger particle sizes imply less dense packing (and hence less efficient use of bed volume) and greater macro-porosity, which aids mass transport. Packing behavior will also affect inter-
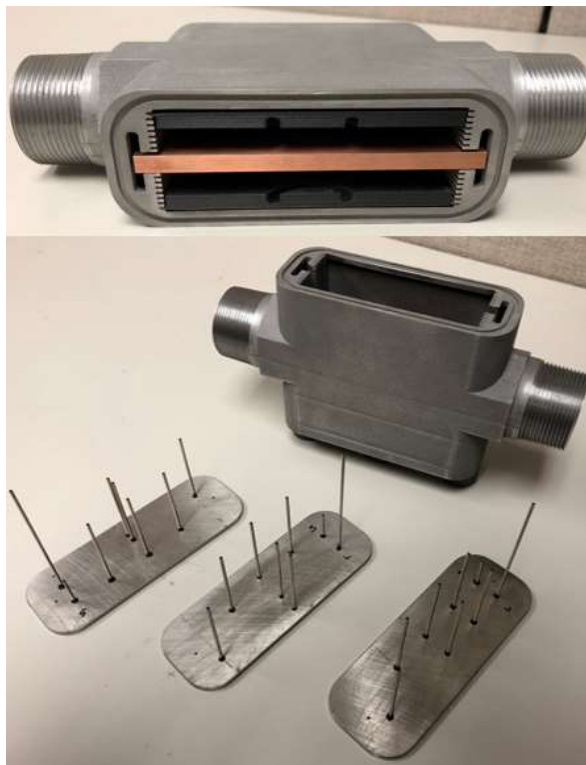

Figure 8. Zeolite 13X in three forms.

pellet contact and heat conduction. The three sizes chosen cover a large range and should reveal any obvious benefits or detriments relative to the aforementioned factors.

Three different bed thicknesses were also chosen, 3.0 mm, 5.2 mm, and 9.3 mm. The smallest of these corresponds approximately to the size of the largest pellet, resulting in a ratio of pellet diameter / bed size ≈ 1, or a monolayer in this extreme case. With the exception of the powder, all bed sizes have significant wall effects due to packing. Even in a full-scale RCAP, wall effects will dominate because large uninterrupted beds lacking any additional conductive "fin" structure cannot be rapidly "swung" between temperature extremes. Any conductive fins will alter the packing.

The temperatures chosen for the heated and chilled baths were 85° C and -20° C respectively. The range fits comfortably within the ambient conditions on Mars and temperatures that may be expected as waste heat streams from other ISRU systems. However, more specific values derived from a larger, systems-based study would be beneficial to future analyses, as Zeolite adsorption and desorption is

Figure 9. Schematic of thermocouple rake. *Thermocouple locations shown in (X,Y) format in millimeters. Color legend corresponds to probe length in millimeters. Liquid flows in the central plate (blue region) from right to left, gas in the bed (gray region) from left to right.*

#	Test	MACS gas	Cold Bath Temp (°C)	Hot Bath Temp (°C)
1	Max bed size, 1/8" pellet	CO2	-20	85
2	Mid bed size, 1/8" pellet	CO2	-20	85
3	Min bed size, 1/8" pellet	CO2	-20	85
4	Max bed size, 1/16" pellet	CO2	-20	85
5	Mid bed size, 1/16" pellet	CO2	-20	85
6	Min bed size, 1/16" pellet	CO2	-20	85
7	Max bed size, 600 mesh	CO2	-20	85
8	Mid bed size, 600 mesh	CO2	-20	85
9	Min bed size, 600 mesh	CO2	-20	85
10	Max bed size, 1/8" pellet	Mars	-20	85
11	Mid bed size, 1/8" pellet	Mars	-20	85
12	Min bed size, 1/8" pellet	Mars	-20	85
13	Max bed size, 1/16" pellet	Mars	-20	85
14	Mid bed size, 1/16" pellet	Mars	-20	85
15	Min bed size, 1/16" pellet	Mars	-20	85
16	Max bed size, 600 mesh	Mars	-20	85
17	Mid bed size, 600 mesh	Mars	-20	85
18	Min bed size, 600 mesh	Mars	-20	85

Figure 10. Proposed test matrix.

very sensitive to temperature. Within the bed itself, temperature is measured at multiple points with a thermocouple rake seen in Figure 7, and laid out in the schematic in Figure 9. Two thermocouples contact the heat exchanger at either end to measure any gradient, the others are distributed throughout the bed to capture the temperature distribution with minimal bed disruption.

The anticipated full test matrix is shown in Figure 10. All three Zeolite geometries will be tested with each bed thickness, and each test replicated three times. Both pure CO_2 and simulated Mars atmosphere are used to isolate effects of undesired N_2 adsorption and any diffusion inhibition caused by the trace gases. Before a test set was run, the Zeolite was heated with the isolation valves open to remove as much ambient water vapor and other species as possible from the pump assembly. A true bakeout would require heating to 200-300° C, but this would not be practical with the current test configuration. Resident species in the sorbent is a serious issue that requires further research and different handling procedures.
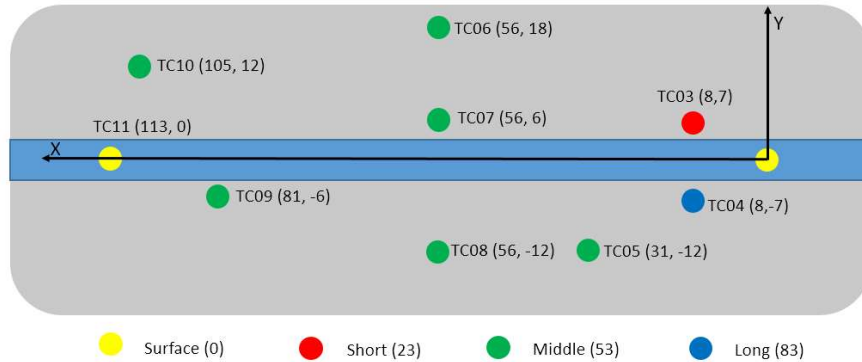
IV. Results and Discussion

A. Concerning Fans

Fans or blowers are required in any large-scale Martian ISRU system to move the process gas (atmosphere) through the equipment until it can be pressurized to a useful density. This includes the pressurization hardware itself, whether it is an adsorption pump or cryofreezer, and any dust filtration subsystem that precedes it. The extremely low density of the Martian atmosphere makes this challenging. ISRU experimental setups frequently sidestep this problem by feeding Mars gas directly into the apparatus to be tested, and pulling a vacuum on the other "side" of it to promote flow. Researchers have also used simple "muffin" or computer cooling axial fans, likely due to their low cost and ease of incorporation in test apparatus. The authors were curious to see how other types of fans may perform under these conditions. No real distinction between a "blower" and a "pump" exists, but for our purposes a blower is a pump using a relatively small amount of power relative to that consumed by the RCAP system as a whole. It serves to enhance convection and related processes, the pressure rise generated is merely incidental.

A blower was incorporated into the RCAP design to increase mass transport in the sorbent bed and help move undesirable gases (N_2 and Ar) out so they did not create a diffusion-inhibiting "blanket." Two different styles were tested, a Jabsco 4.25" (10.8 cm) diameter centrifugal blower and a Sanyo Denki 92x25 mm axial fan. Both were attached with converging fairings to the PVC ducting visible in Figure 4. To measure total pressure generated by the blower, one of the Setra ASM pressure transducers was placed in the middle of the duct in a "ram" configuration, with the sensor port pointing into the flow. The sensor body itself blocks approximately 80% of the flow area of the duct. Using a minimally invasive pressure probe is more typical for this type of measurement, but given the obstructive nature of the RCAP flow-through bed design, blower performance in this configuration was more relevant to experiment operation. The goal was not precise performance characterization of the fans, as the measurements are at the low end of the transducer's range, and the apparatus was not designed for this test, so absolute conclusions should not be drawn. However, as a relative comparison between blower types for this and similar setups, there is value.
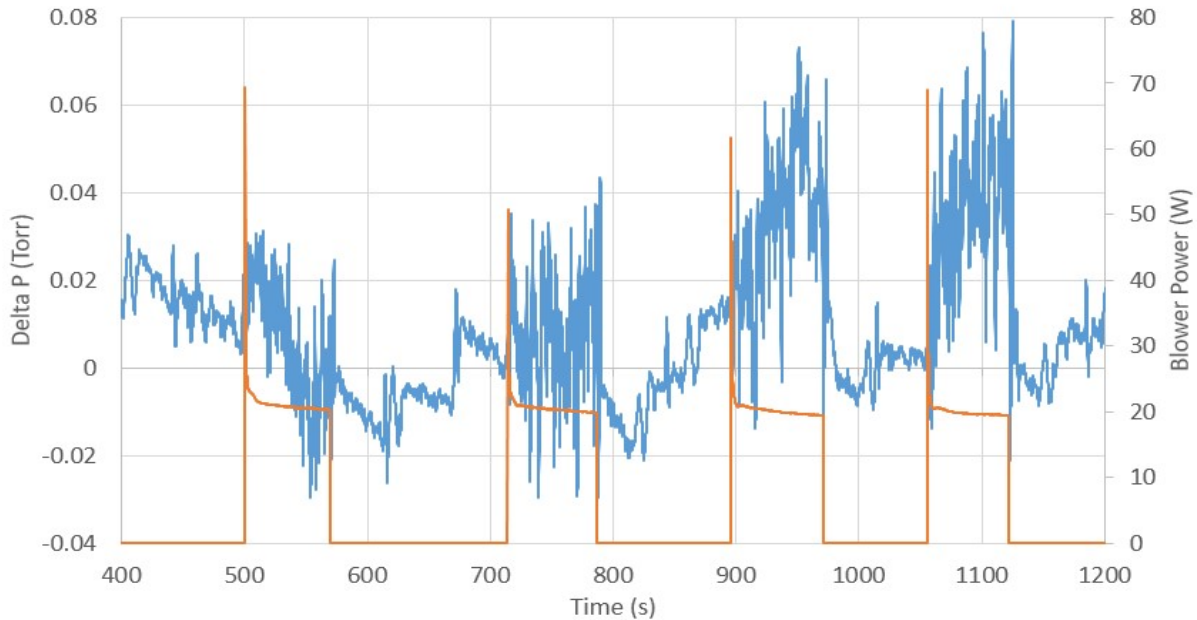

Figure 11. Total pressure delta P from centrifugal blower. *Delta P is in blue (left axis), blower power is in orange (right axis). Pressure results have been averaged to reduce noise. The test portion from 400-1200 s contains four periods of fan activity.*

Tests were run with pure CO_2 at 6-10 Torr in the MACS chamber. Power was monitored via the LabVIEW-GPIB interface with the DC power supply. Due to pressure fluctuations in the chamber caused by the pressure controller algorithm, the vacuum pump and active pressure control were deactivated once 5 Torr was reached. The resulting linear pressure rise was subtracted from the raw measurement to yield a delta pressure. The results from the centrifugal blower are shown in Figure 11. The average delta P over all the blower "on" periods is only 0.02 Torr, which is within the error of the transducer. However, there is a visible distinction between the periods when the blower is active

relative to inactive. Also, a small tape "telltale" placed near the duct exit exhibited irregular motion, indicating some flow was generated by the centrifugal blower.

The performance of the axial blower in shown in Figure 12. The axial fan produces an averaged delta P of 0.13
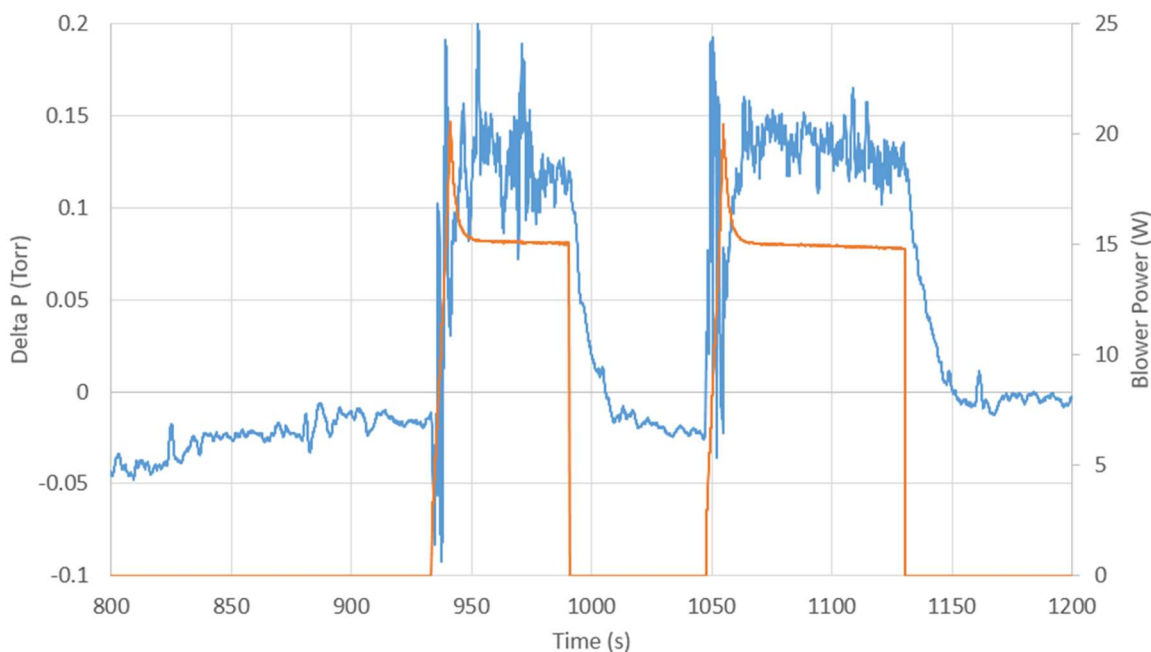

Figure 12. Total pressure delta P from axial blower. *Delta P is in blue (left axis), blower power is in orange (right axis). Pressure data have been averaged to reduce noise. The period from 800 – 1200 s contains two periods of fan activity.*

Torr, which while still on the order of the transducer error, is clearly distinguished from the centrifugal type. Some of this difference may be accounted for by a reduction in vibration reaching the sensor, but the visual comparison is stark. As the axial blower produced approximately 7x the total pressure while using 25% less power, we decided to use it in the test configuration. Development of an axial blower exclusively for Mars, with tailored airfoil shapes and mechanical design, should be an area of work for the ISRU community.

B. Select Preliminary Cycle Results

Testing of the RCAP is currently in progress, but preliminary results from two contrasting cases in the test matrix are included here. Cases #1 and #6 (refer to Figure 10) demonstrate the differences between the thickest and thinnest beds and two pellet sizes. Both tests used only CO_2, and only show a single "Cold-Hot" cycle. This was due to performance limitations of the current chiller and heated bath, which prevented longer runs. We are striving to address these deficiencies, as long transients in sorbent behavior and heat transfer are important for evaluating realistic operation. Nonetheless, some interesting details can be observed even from a limited data set.

Figure 13 presents temperature data from Case #1 during a bakeout/adsorb/desorb cycle. The bed was initially heated (0-50 minutes) with the isolation valves open and no CO_2 flowing into the chamber to help liberate unwanted remnant species from the bed and show bed heating behavior when no desorption is occurring. The isolation valves were later closed, and the CO_2 flow was activated and chamber pressure allowed to stabilize between 6-9 Torr. It is noted that the liquid temperature of the heated bath remained at 85°C from ~30 minutes onward, but the liquid inflow never got above 50°C. This is likely due to heat leaks in the plumbing and the associated thermal mass of adjacent valves and other hardware. While the apparatus could be optimized through use of polymer plumbing and similar modifications to reduce parasitic thermal masses, the difficulty of maintaining working fluid temperature is relevant to a full scale flight RCAP unit, which will likely be harvesting heat from waste streams. The peak ~10°C difference in inflow and outflow temperature can be attributed to both the thermal mass of the plate and heat transfer into the bed, which continued at a nearly constant rate until the cooling phase began. An increased fluid flow rate from a higher performance pump would reduce this temperature delta and increase heat transfer to the bed.

Cooling starts at 50 minutes into the run. The isolation valves were opened and blower activated when the average bed temperature had begun to fall. The subsequent rise in temperature across the bed and the liquid outflow as adsorption began is visible before overall cooling dominates. Cold liquid flow into the RCAP continued for 30 minutes. It is clear due to fluctuations in the inflow temperature that the chiller was not providing consistent cooling, which limits the interpretation of the results during this phase.
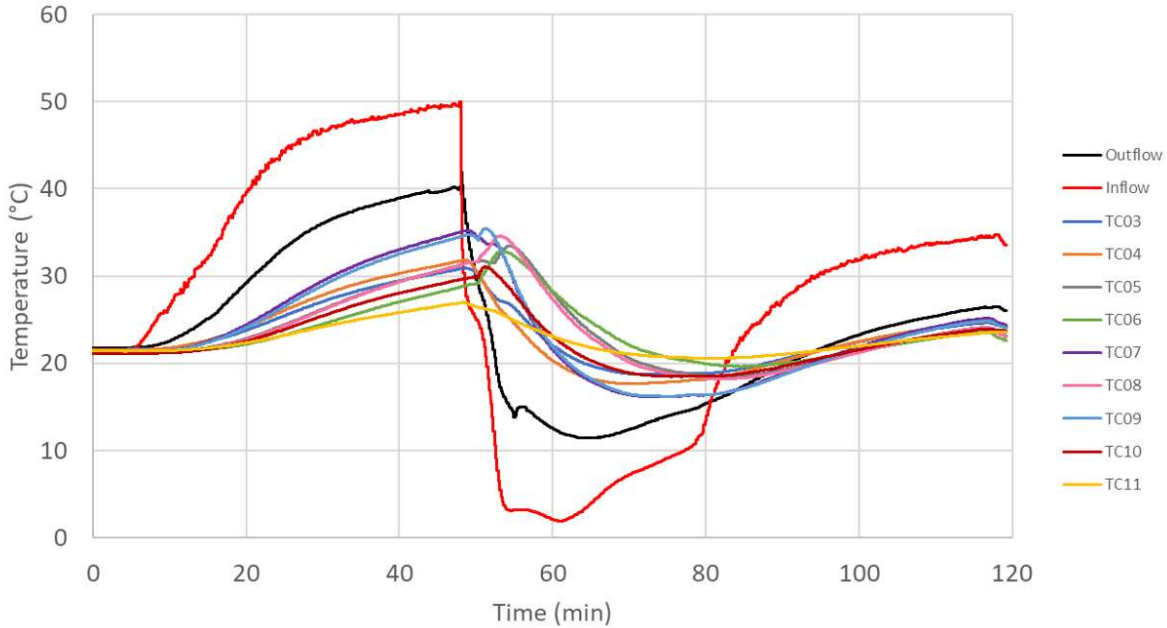

Figure 13. Case #1 temperature results during adsorption. *Heat exchanger plate inflow and outflow liquid temperatures and thermocouples within the bed during a bakeout/adsorb/desorb cycle.*
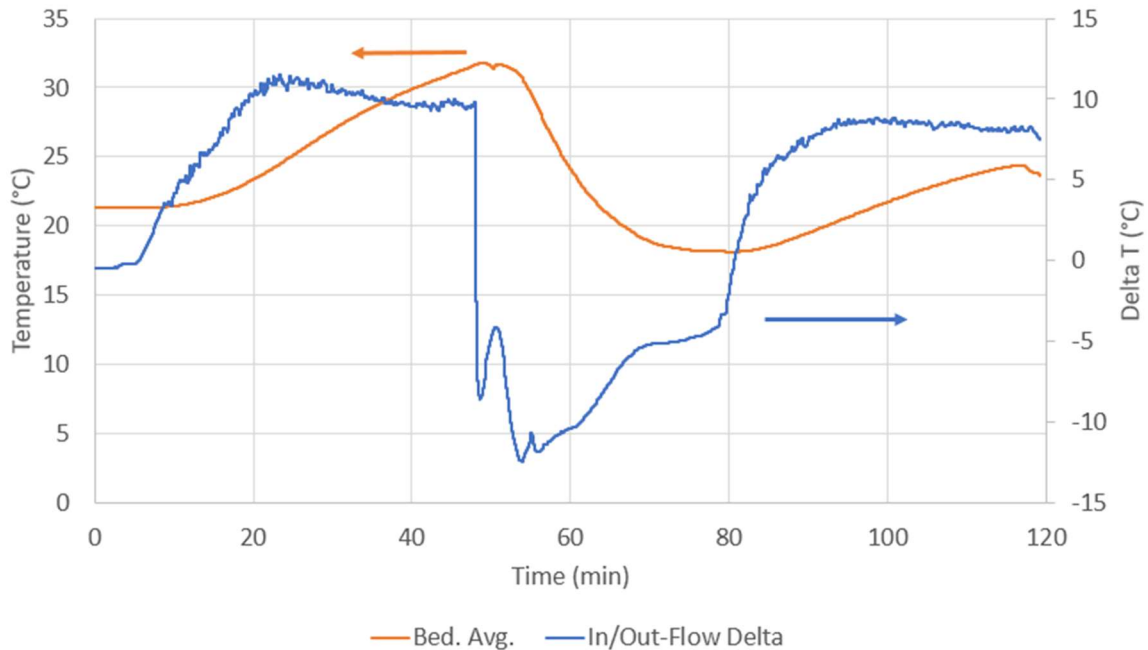

Figure 14. Case #1 average bed temperature and liquid inflow/outflow temperature difference. *Bed temperature (left axis) and the inflow/outflow delta (right axis).*

Within the bed, temperatures differed by up to ~5°C, with TCs 07 and 09, both nearest the plate, following the plate most quickly while TC06 (furthest away) predictably lagged the most. TC11, meant to touch the plate directly,

9

was likely making poor contact and is probably most representative of the RCAP outer wall. Comparing TCs 07 and 09 with TCs 05 and 08, the 6 mm difference in distance from the central plate creates a ~4°C difference in temperature during heating that is notably less distinct once adsorption begins. This suggests that the mass transfer gradients in the bed are less severe than the heat transfer gradients, as CO_2 can readily adsorb at and hence heat these locations deeper in the bed, despite their relative distance from the plate.

Figure 14 plots the total averaged bed temperature across TCs 03-10 and the difference between liquid inflow and outflow temperatures during heating and cooling. The averaged bed temperature swing was only ~6°C, demonstrating the challenges to effective heat transfer in insulating sorbent beds. During both heating and cooling, the temperature gradient across the plate was ~9°C.
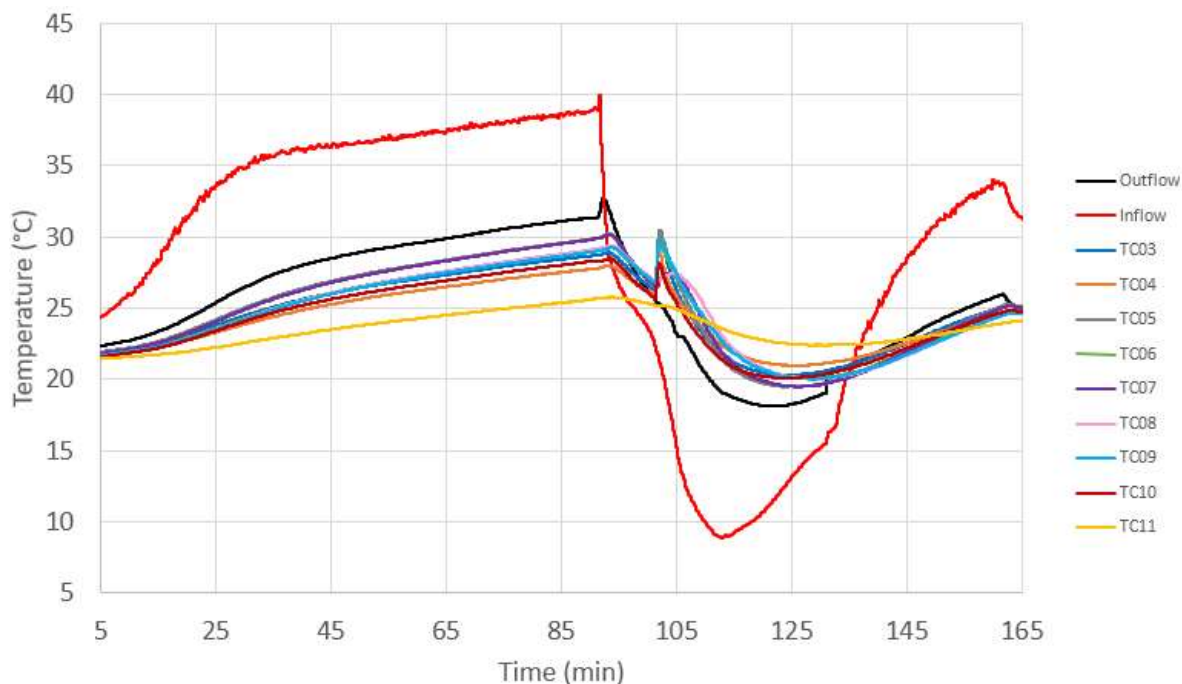

Figure 15. Case #6 temperature results during adsorption. *Heat exchanger plate inflow and outflow liquid temperatures and thermocouples within the bed during an adsorb/desorb cycle. The first five minutes have been trimmed to focus on active portion of test.*

Figure 15 depicts the corresponding temperature results for Case #6, also with 30 minute adsorption and desorption phases. The much thinner bed obviously leads to much less temperature variance throughout, only ~2°C. Some qualitative differences are also observed relative to Case #1. TC07 now follows the central plate most quickly, while TC04 lags. However, these distinctions more difficult to interpret due to the compressed bed thickness. Future data points, and properly performing support hardware will reveal additional phenomena. It is also noted that the bed took longer to heat initially and the liquid inflow temperature only reached a 39°C maximum. Likewise, the lowest cooling liquid temperature was only ~8°C, and showed the same inconsistency seen during Case #1. Stable, reliable source temperatures are a necessary goal as we refine the experimental setup and continue testing.
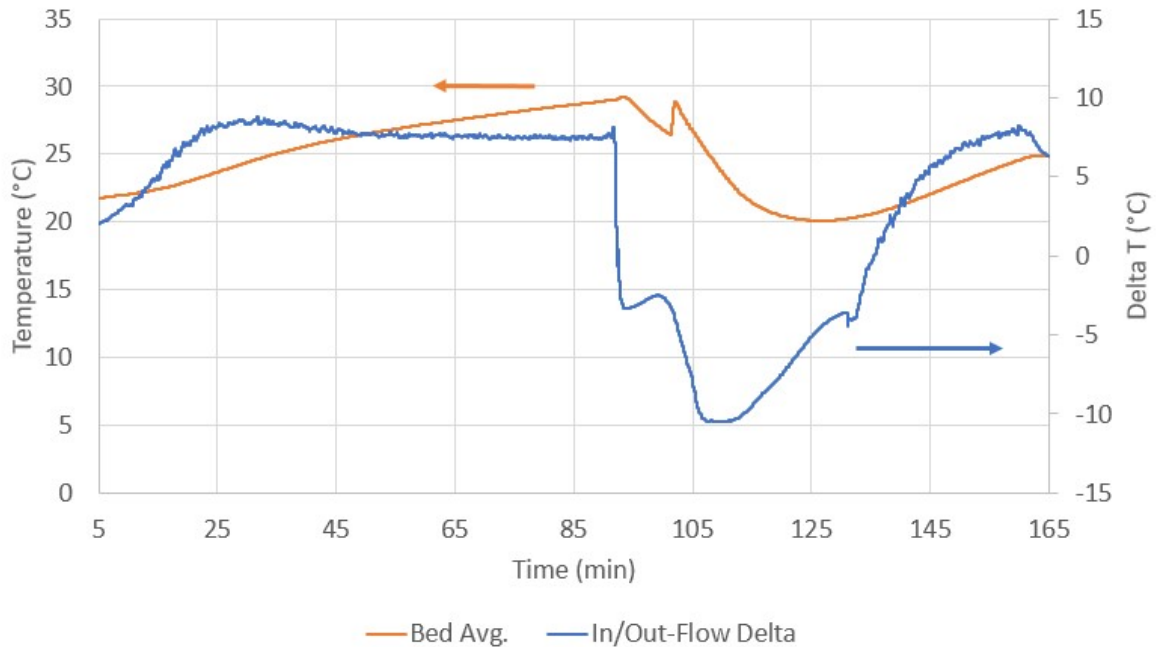
Figure 16. Case #6 average bed temperature and liquid inflow/outflow temperature difference. *Bed temperature (left axis) and the inflow/outflow delta (right axis).*

Figure 16 shows the average bed temperature and liquid inflow and outflow temperature delta for Case #6. Despite a thinner, and ostensibly lower thermal mass bed, the average temperature swing was only ~5°C over the cooling and heating phases. This is attributed to less extreme driving liquid temperatures. The liquid temperature delta across the plate was similar to Case #1.

Given that the RCAP is a pump, the most important results should be measurements of internal pressure during the desorption phase and mass flows of the product species. However, the small temperature swing of the bed currently observed during testing only leads to a small amount of CO_2 being released and a ~1 Torr (~15%) increase in internal pressure relative to ambient. Future work will enhance the capabilities of the test configuration and vary the adsorption and desorption phase times to increase production.

V. Conclusion

The RCAP stands as an appealing technology for CO_2 collection and compression and the first in a chain of linked processing steps for effective ISRU on Mars. The tests thus far underline the anticipated limitations of rapid temperature cycling, and provide guidance for continued experimentation and modeling. With better models, more adventurous geometries could be designed that boost overall sorbent bed performance. Conduction augmentation with additional fin-like structures or conductive shot is attractive[16], but there is reason to doubt its efficacy when evaluated holistically as part of a system. Besides displacing sorbent mass, these structures could negatively influence gas flow by blocking it or allowing it to "channel" along a wall and bypass a large portion of the bed.

It must be noted that there is a limit on the performance of the RCAP since the adsorption process is heavily dependent on both pressure and temperature. Eventually, as the pressure within the RCAP is increased, it becomes more favorable for CO_2 molecules to adsorb rather than desorb despite the sorbent being heated. In order to maintain the same specific productivity, therefore, more adsorbent mass be added and/or a higher desorption temperature would be required. It follows that each RCAP configuration – whether more adsorbent is used or if the boundary conditions become more favorable – will have a maximum achievable pressure ratio. This means that the RCAP has the potential for becoming a massive and power hungry system that may require diurnal cycles for Martian applications – in which case, the pump will no longer be considered "rapid."

It is for this reason why staging, or using multiple RCAPs in series, is clearly an attractive method since it allows each successive stage to boost the CO_2 pressure to the desired value without encountering the pressure limit. For the case of Martian applications, this may be the most appropriate path for adsorption beds as the total system mass can be reduced while boosting specific productivity for the range of desired pressure ratios[6,17]. In addition, the designer can now use multiple sorbents with characteristics targeted for different pressures. For example, the first stage of the

system can employ a sorbent with desirable qualities in the lower pressure regime while the later stages can select sorbents tailored for the higher pressure targets. Such a design selection, consequently, will result in reduced bed mass, and a possible reduction in the energy required to run the thermodynamic cycle depending on the sorbents used.

The design choices provided by staging, therefore, offer a larger design space to make rapid cycling more feasible; however, one must not forget the added complexity and penalties that come with it. With the addition of staging, the ideal thermodynamic cycle shown in Figure 1 must be synced and adjusted to account for the transfer of CO_2 to each stage. Since additional volume is added as a result of the interstage CO_2 valve network, knowledge of the pressurization within and between each stage becomes paramount. The determination of these interstage pressures, and subsequently the highest pressure achieved within each stage, will ultimately decide whether feasibility is assured or not. Therefore, careful design must be conducted to effectively size the entire RCAP to be robust and reliable.

It should not be overlooked, however, that staging will add parasitic thermal mass. The result of the additional valves, structural elements and sensors will drive the total cycle time to be increased; thereby, driving the designer to seek out better designs and better performing sorbents to drive down mass and power costs. To characterize the performance of an additional stage, testing is also planned on a two-stage RCAP where the second stage has nearly identical geometry of the first. The results of this test will be used to inform current models.

With data from a larger-scale experiment, better systems engineering decisions can be made regarding comparisons to other compression technologies. To maximize mass and energy efficiency, the RCAP concept requires input from the larger ISRU and mission design community, as packaging and techniques like waste heat utilization and recuperation are dependent on choices made by the surrounding hardware. The available driving temperatures (hot and cold) will be critical to whether an RCAP can function practically and yield sufficient CO_2. With further development and smart integration into a commodity production plant, the RCAP could help unlock the Martian surface.

Acknowledgments

References

[1]Yang, Ralph T., *Gas Separation by Adsorption Processes,* Butterworth Publishers, Stoneham, 1987.

[2]Frisbee, R. H., "Mass and Power Estimates For Mars In-Situ Propellant Production Systems," AIAA/SAE/ASME/ASEE 23rd Joint Propulsion Conference, AIAA-87-1900, San Diego, CA, 1987.

[3]Ramohalli, K., Lawton, E., Ash, R., "Recent Concepts in Missions to Mars: Extraterrestrial Processes," *Journal of Propulsion*, Vol. 5, No.2, 1989, pp.181-187.

[4]Finn, J. E., "Low-Power Temperature-Swing Adsorption for Mars Atmosphere Acquisition," *ISRU III Technical Interchange Meeting*, 1999.

[5]"Laboratory Directed Research and Development Annual Report – Fiscal Year 2000," Pacific Northwest National Laboratory, PNNL-13501, 2001.

[6]Brooks, K.P., Rassat, S.D., TeGrotenhuis, W.E., "Development of a Microchannel In Situ Propellant Production System," Pacific Northwest National Laboratory, PNNL-15456, 2005.

[7]Linne, D.L., Gaier, J.R., Zoeckler, J.G., Kolacz, J.S., Wegent, R.S., Rassat, S.D., Clark, L.D., "Demonstration of Critical Systems for Propellant Production on Mars for Science and Exploration Missions," *51st AIAA Aerospace Sciences Meeting*, Grapevine, TX, 2013.

[8]Li, X.H., Hou, X.H., Zhang, X., Yuan, Z.X., "A review on development of adsorption cooling – Novel beds and advanced cycles," *Energy and Conversion Management*, Vol. 94, 2015, pp. 221-232.

[9]Rezk, A., Al-Dadah, R.K., Mahmoud, S., Elsayed, A., "Effects of contact resistance and metal additives in finned-tube adsorbent beds on the performance of silica gel/water adsorption chiller," *Applied Thermal Engineering*, Vol. 53, 2013, pp. 278-284.

[10]Kleinhenz, Julie E., Paz, Aaron. "An ISRU Propellant Production System to Fully Fuel a mars Ascent Vehicle" 10th Symposium on Space Resource Utilization, AIAA 2017-0423, Grapevine, TX, 2017.

[11]N'Tsoukpoe, K.E., Restuccia, G., Schmidt, T., Py, X., "The size of sorbents in low pressure sorption or thermochemical energy storage processes," *Energy*, Vol. 77, 2014, pp. 983-998.

[12]Afandizadeh, S., Foumeny, E.A., "Desing of packed bed reactors: guides to catalyst shape, size, and loading selection," *Applied Thermal Engineering*, Vol. 21, 2001, pp. 669-682.

[13]Benyahia, F., O'Neill, K.E., "Enhanced Voidage Correlations for Packed Beds of Various Particle Shapes and Sizes," *Particulate Science and Technology*, Vol. 23, 2005, pp.169-177.

[14]Cheng, P., Vortmeyer, D., "Transverse thermal dispersion and wall channeling in a packed bed with forced convective flow," *Chemical Engineering Science*, Vol. 43, No. 9, 1988, pp. 2523-2532.

[15]Schunk, G.R., Peters, W.T., Thomas Jr., J.T., "Four Bed Molecular Sieve – Exploration (4BMS-X) Virtual Heater Design and Optimization," *47th International Conference on Environmental Systems*, Charleston, South Carolina, 2017.

[16]Verde, M., Harby, K., Coberan, J.M., "Optimization of thermal design and geometrical parameters of a flat tube-fin adsorbent bed for automobile air-conditioning," *Applied Thermal Engineering*, Vol. 111, 2017, pp. 489-502.

[17]Hasseeb, H., Iannetti, A., "A System Level Mass and Energy Calculation for a Temperature Swing Adsorption Pump used for In-Situ resource Utilization (ISRU) on Mars," Thermal Fluids Analysis Workshop, NASA Marshall Space Flight Center, AL, 2017.